

Why 11-*cis*-Retinal? Why Not 7-*cis*-, 9-*cis*-, or 13-*cis*-Retinal in the Eye?

Sivakumar Sekharan[†] and Keiji Morokuma^{*,†,‡}

[†]Cherry L. Emerson Center for Scientific Computation and Department of Chemistry, Emory University, Atlanta, Georgia 30322, United States

[‡]Fukui Institute for Fundamental Chemistry, Kyoto University, 34-4 Takano, Nishihiraki-cho, Kyoto 606-8103, Japan

S Supporting Information

ABSTRACT: One of the basic and unresolved puzzles in the chemistry of vision concerns the natural selection of 11-*cis*-retinal as the light-sensing chromophore in visual pigments. A detailed computational examination of the structure, stability, energetics, and spectroscopy of 7-*cis*-, 9-*cis*-, 11-*cis*-, and 13-*cis*-retinal isomers in vertebrate (bovine, monkey) and invertebrate (squid) visual pigments was carried out using a hybrid quantum mechanics/molecular mechanics (QM/MM) method. The results show that the electrostatic interaction between retinal and opsin dominates the natural selection of 11-*cis*-retinal over other *cis* isomers in the dark state. In all of the pigments, 9-*cis*-retinal was found to be only slightly higher in energy than 11-*cis*-retinal, which provides strong evidence for the presence of 9-*cis*-rhodopsin in nature. 7-*cis*-Retinal is suggested to be an “upside-down” version of the all-*trans* isomer because the structural rearrangements observed for 7-*cis*-rhodopsin from squid were found to be very similar to those for squid bathorhodopsin. The progressive red shift in the calculated absorption wavelength (λ_{\max}) (431, 456, 490, and 508 nm for the 7-*cis*-, 9-*cis*-, 11-*cis*-, and 13-*cis*-retinal isomers) is due to the decrease in bond length alternation of the retinal.

Rhodopsin, the visual pigment found in the rod outer segments of the vertebrate and invertebrate photoreceptor, mediates the transformation of light into vision.¹ Bovine and squid rhodopsin belong to the class of vertebrate and invertebrate photoreceptors,² respectively, and are also the only members of the G_t and G_q signaling type of G-protein coupled receptors (GPCRs) with a known X-ray structure.³ The heptahelical membrane protein is composed of a light-absorbing 11-*cis*-retinal chromophore covalently bound to the ϵ -amino group of a lysine residue of an apoprotein (opsin) via a protonated Schiff base (PSB11) linkage (Figure 1). The positive charge of the chromophore is balanced by the negative charge of the glutamate counterion. Glu113 serves as a H-bonded counterion in bovine rhodopsin,⁴ while Glu180 serves as a non-H-bonded counterion in squid rhodopsin.⁵ Remarkably, irrespective of the difference in their H-bonding schemes, the two counterions cause a strong blue shift of ~ 120 nm in the first ($S_0 \rightarrow S_1$) vertical excitation energy λ_{\max} (all values in nm) of PSB11 in going from the gas phase (exptl = 610; calcd = 616/604) to the protein environments (exptl = 498, calcd = 495 in bovine; exptl = 488, calcd = 490 in squid).⁵



Figure 1. Schematic representation of 7-*cis*- (PSB7, green), 9-*cis*- (PSB9, blue), 11-*cis*- (PSB11, black), 13-*cis*- (PSB13, purple), and all-*trans*-retinal (PSBT, red). R refers to Lys-305 in squid and Lys-296 in bovine and monkey rhodopsins.

7-*cis*-Rhodopsin is an artificial analogue of rhodopsin that contains the protonated Schiff base of 7-*cis*-retinal (PSB7) as its chromophore. It is characterized by its low reaction rate for pigment formation, low thermal stability, and strongly blue-shifted λ_{\max} (exptl = 450) relative to the 11-*cis* isomer (exptl = 498) in bovine.⁶ 9-*cis*-Rhodopsin (isorhodopsin), the most studied analogue of rhodopsin, contains the protonated Schiff base of 9-*cis*-retinal (PSB9) as its chromophore. It undergoes a bleaching sequence identical to that of rhodopsin and is characterized by a weakly blue-shifted λ_{\max} in both the vertebrate (exptl = 485 in bovine)⁷ and invertebrate (exptl = 465 in squid) pigments.⁸ Because both PSB9 and PSB11 can bind to opsin and form pigments with distinct spectral properties, PSB9 is often used as an artificial analogue to probe the structure and function of native rhodopsin.⁹

13-*cis*-Rhodopsin, a less-studied isomer of the visual pigments, is another artificial analogue of rhodopsin that contains the protonated Schiff base of 13-*cis*-retinal (PSB13) bound to the opsin. Because of the difficulties involved in synthesizing the pure form of 13-*cis*-rhodopsin, earlier studies could incorporate only 9,13-di-*cis* (as it already contains the 9-*cis* configuration) or a locked form of 13-*cis* (not the pure form of 13-*cis*) into bovine opsin.¹⁰ In fact, archae- and proteorhodopsins were found to contain mixtures of all-*trans* (PSBT) and 13-*cis* isomers in the dark, because they are completely different protein families,

Received: September 18, 2011

Published: October 25, 2011

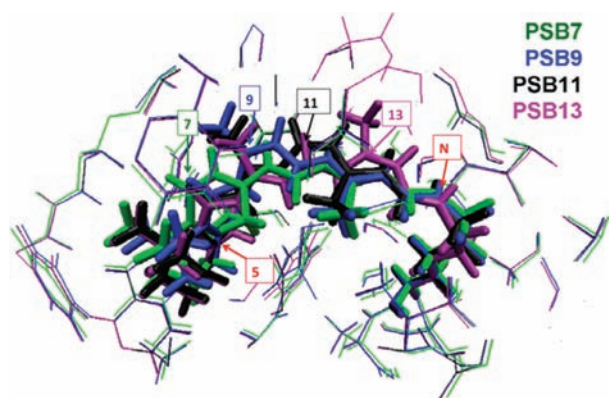


Figure 2. QM/MM-EE optimized geometries of the retinal binding pockets containing PSB7 (green), PSB9 (blue), PSB11 (black), and PSB13 (purple) models.

where the binding site has been optimized for the all-*trans* and 13-*cis* isomers.¹¹ Apparently, in the visual pigments only PSB11 has been found to be present in the dark.¹² Since the primary event in vision involves no breaking of chemical bonds but only a change in the shape of the molecule from bent 11-*cis* to distorted all-*trans*, one wonders why the reactant is always 11-*cis* and not 7-*cis*, 9-*cis*, or 13-*cis*? Theoretical and experimental studies have argued that the nonbonded interaction between the C10–H and C13–Me groups can facilitate efficient, ultrafast, and stereoselective isomerization of the 11-*cis* isomer to the all-*trans* isomer.¹³ However, in the absence of direct evidence from pigments containing the pure forms of the PSB7 and PSB13 isomers, resolving the fundamental question concerning the natural selection of PSB11 still remains an open question.

In light of the exponential development of theoretical methods and computational resources, we are now in a position to prepare models of visual pigments across different parts of the animal kingdom. In particular, comparative analysis of the structure, stability, energetics, and spectroscopy of retinal isomers in vertebrate and invertebrate visual pigments can be performed using hybrid quantum mechanics/molecular mechanics (QM/MM) methods.¹⁴ In such methods, a relatively small region of the system in which chemical reactions and spectroscopy occur is modeled at the QM level, and the remaining part is treated with MM force fields. By employing one such method, the ONIOM (Our own N-layered Integrated Molecular Orbital) QM/MM protocol,¹⁵ we aimed to provide insights into the dark side of vertebrate and invertebrate rhodopsins.

The QM/MM-optimized structures of wild-type bovine and squid rhodopsin, in which the retinal (PSB11) is treated via QM and the opsin containing 348 (in bovine) or 448 (in squid) amino acids is treated via MM, were taken from refs 5 and 16. To probe the impact of evolutionary displacement of amino acid positions in the natural selection of PSB11, we also modeled monkey rhodopsin, which contains 22 different amino acids (22/348) in comparison with bovine rhodopsin.¹⁷ Details of the optimization method and optimized structures are given in the Supporting Information (SI).

Although all of the retinal isomers are incorporated into an identical binding site (Figure 2), geometry optimization (see below) allows relaxation of the immediate environment that may stabilize or destabilize PSB7/9/13 relative to PSB11, as originally proposed by Birge et al.¹⁸ Especially as the *cis* conformation is present at different positions of polyene side chain for the

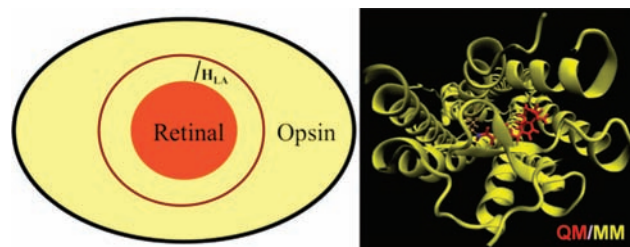


Figure 3. Schematic representation of the two-layer ONIOM (QM:MM) scheme employed in this study. The retinal treated in the QM part (red circle) is connected to the opsin (yellow) via a hydrogen link atom (H_{LA}).

different retinal isomers (at the beginning for PSB7, in-between for PSB9, in the middle for PSB11, and at the very end for PSB13), binding to the opsin induces significant nonplanar distortions in the retinal. Also, the retinal backbone appears to be perpendicular to the plane of the β -ionone ring for PSB7 and PSB13. As a result, the lengths of the retinal conjugation (from C5 to the Schiff base N^+) for PSB7 and PSB13 are similar (~ 10.85 Å), while it is shorter by 0.24 Å for PSB11 (10.61 Å) and 0.40 Å for PSB9 (~ 10.45 Å). Because of the steric interaction between the C5–Me and C9–Me groups, the C6–C7–C8 angle widens and creates the space required for fitting PSB7 into the binding pocket. Apparently, the conformational distortions induced in PSB7 are analogous to those found from NMR measurements on 10Me-PSB11 analogues.¹⁹ In 10Me-PSB11, the C10–Me and C13–Me groups interact with each other to induce out-of-plane distortions, which increase the distance between the C10–Me and C20–Me positions (i.e., from 3.04 Å in PSB11 to 3.47 Å in 10Me-PSB11). This property can be compared to the increase in distance between C6–Me and C19–Me position (i.e., from 2.66 Å in PSB11 to 3.00 Å in PSB7).

All QM/MM calculations in this study were performed using the two-layer ONIOM (QM:MM) scheme, in which the QM part contains the full retinal and the MM part contains the full opsin, depicted as point charges plus van der Waals interactions; the interface between the QM and MM regions was treated by the hydrogen link atom (Figure 3). The total energy of the system was obtained as ${}^{EE}E$, the energy in the electronic embedding (EE) scheme, in which the QM:MM interaction is included in the QM calculation and therefore the QM wave function is polarized by the MM point charges. Throughout this study, we employed for geometry optimization the QM/MM-EE scheme, in which the retinal and all of the amino acid residues and water molecules within a radius of 4 Å from any chromophore atom were optimized while the other atoms were fixed at their positions in the wild-type structure. An alternative QM:MM energy is ${}^{ME}E$, the energy in the mechanical embedding (ME) scheme, in which the QM:MM interaction is calculated in the classical Hamiltonian and the wave function is not polarized.²⁰

Lugtenburg and Mathies have shown that control of the photochemical reaction by the ground-state conformation is achieved through the induced fit of the retinal in rhodopsin.²¹ To disentangle the factors that contribute to the stabilization of 11-*cis*-retinal relative to the induced misfit of other retinal isomers into rhodopsin, we performed the following analysis of the relative energy of each isomeric form of rhodopsin. At the above-mentioned EE-optimized geometry of each rhodopsin, the

Table 1. Evaluation of the Role of Opsin in the Natural Selection of PSB11 in Visual Pigments Using the Values of ${}^{\text{ME}}E_{\text{QM}}$, E_{DEF} , ${}^{\text{ME}}E_{\text{MM}}$, ${}^{\text{ME}}E$, and ${}^{\text{EE}}E$ for Different Isomer Rhodopsins Relative to the Corresponding Values for PSB11 in Vertebrate (Bovine, Monkey) and Invertebrate (Squid) Pigments (See the SI for Details)

model	${}^{\text{ME}}E_{\text{QM}}(E_{\text{DEF}})/{}^{\text{ME}}E_{\text{MM}}/{}^{\text{ME}}E/{}^{\text{EE}}E$ (kcal/mol)		
	bovine	monkey	squid
PSB7	5.3(4.2)/8.1/13.4/10.8	5.4(4.3)/7.8/13.2/11.4	9.0(7.9)/3.1/12.1/12.2
PSB9	-3.1(0.1)/5.9/2.8/0.9	-2.9(0.3)/4.9/1.9/0.8	-2.4(0.8)/2.9/0.5/2.1
PSB11	0.0(0.0)/0.0/0.0/0.0	0.0(0.0)/0.0/0.0/0.0	0.0(0.0)/0.0/0.0/0.0
PSB13	3.1(6.2)/27.9/31.0/28.4	8.9(12.0)/28.9/37.8/35.2	-1.2(1.9)/16.8/15.5/15.8

single-point values of ${}^{\text{ME}}E$ and ${}^{\text{EE}}E$ were calculated. The difference between ${}^{\text{EE}}E$ and ${}^{\text{ME}}E$ comes mainly from the polarization of the retinal chromophore by the MM charges of the opsin. ${}^{\text{ME}}E$ can be divided into the QM energy of retinal alone at the rhodopsin-optimized geometry (${}^{\text{ME}}E_{\text{QM}}$) and the MM contributions from opsin and its interaction with retinal (${}^{\text{ME}}E_{\text{MM}}$):

$${}^{\text{ME}}E = {}^{\text{ME}}E_{\text{QM}} + {}^{\text{ME}}E_{\text{MM}}$$

$${}^{\text{ME}}E_{\text{MM}} = {}^{\text{ME}}E_{\text{MM}}(\text{opsin}) + {}^{\text{ME}}E_{\text{MM}}(\text{retinal-opsin})$$

${}^{\text{ME}}E_{\text{QM}}$ is higher than the energy of retinal at its gas-phase-optimized geometry, and the difference represents the deformation energy of retinal in the protein (E_{DEF}):

$$E_{\text{DEF}} = {}^{\text{ME}}E_{\text{QM}} - E_{\text{QM}}(\text{gas-phase retinal})$$

In Table 1, we list for each protein the values of ${}^{\text{ME}}E_{\text{QM}}$, E_{DEF} , ${}^{\text{ME}}E_{\text{MM}}$, ${}^{\text{ME}}E$, and ${}^{\text{EE}}E$ for each rhodopsin isomer relative to the corresponding values for the reference 11-*cis* isomer.

In all of the animal pigments in terms of the ultimate EE energy (${}^{\text{EE}}E$), the rhodopsin with PSB11 is the most stable, followed closely by PSB9 (higher by 0.8–2.1 kcal/mol); PSB7 and PSB13 are very unstable, and the overall order of stability is PSB11 > PSB9 > PSB7 > PSB13. The fact that PSB9 is only slightly higher in energy than PSB11 across all pigments provides evidence for the presence of 9-*cis*-rhodopsin in nature. The analysis using Table 1 provides further insight into the origin of this stability order. One notices that this order is well-maintained in ${}^{\text{ME}}E$. The difference between ${}^{\text{EE}}E$ and ${}^{\text{ME}}E$, the energy due to the polarization of the chromophore wave function by the protein electrostatic potential, is at most ~ 2 kcal/mol and is not important. In contrast, the order of stability is significantly altered if we compare only the energies of PSB retinals (PSBRs) in protein (${}^{\text{ME}}E_{\text{QM}}$). In this case, the order of stability is PSB9 > PSB11 > PSB7 > PSB13, with the exception of squid, where the order is PSB9 > PSB11 > PSB13 > PSB7. The stability of PSB13 over PSB7 in squid may be related to the position of the counterion, which when H-bonded to the retinal (as in bovine/monkey) may destabilize PSB13 more than PSB7. However, it is important to recognize that PSB9 is more stable than PSB11 with respect to ${}^{\text{ME}}E_{\text{QM}}$. Interestingly, molecular dynamics studies of deep-red cone pigments have found PSB9 to be more stable than PSB11.²² Recently, experimental studies have also shown 9-*cis*-13-isopropylretinal to act as a superagonist after illumination and that the opsin binding site shows preference for 9-*cis* analogues over 11-*cis* analogues.²³ Further, while some analogues of the 9-*cis* isomer perform better than their 11-*cis* counterparts, there is abundant evidence in the literature that this is usually not the case.

The energies of the isomeric forms of retinal optimized in the gas phase (without the protein) have the following order of stability: PSB9 (−3.2 kcal/mol) > PSB13 (−3.1) > PSB11 (0.0) > PSB7 (5.3). This means that in the gas phase, PSB9 and PSB13 are more stable than the naturally occurring (in protein) PSB11; PSB7 is intrinsically unstable because of the steric interaction between the C5–Me and C9–Me groups, as mentioned above. Of course, this argument is a little biased, as the naturally occurring protein is optimized in evolution to stabilize PSB11. PSB13 fits poorly in this protein, making the energy of the protein plus the chromophore higher than that for PSB11. PSB9 fits well to a certain extent, although the energetic advantage over PSB11 in the gas phase is lost.

To calculate the λ_{max} of PSBR geometries in both the gas phase (QM only) and in protein environments (QM/MM), the spectroscopic-oriented configuration interaction method²⁴ with the +Q Davidson correction (SORCI+Q) and the 6-31G* basis set was used (Table 2). For the *planar cis*-PSBR isomers in vacuo, where the retinal is cut off from any external environmental perturbation, the calculations yielded an average value ($\Delta\lambda$) of ~ 610 nm²⁵ (7-*cis*, 591; 9-*cis*, 615; 11-*cis*, 625; 13-*cis*, 623). However, for the distorted structure of retinal in the protein environment, the calculated λ_{max} is considerably blue-shifted in both the gas phase (7-*cis*, 553; 9-*cis*, 566; 11-*cis*, 611; 13-*cis*, 623) and the protein environment [7-*cis*, 431; 9-*cis*, 456; 11-*cis*, 490; 13-*cis*, 508). The origin of the progressive red shift going from 7-*cis* to 13-*cis* can be traced back to the decrease in the average bond-length alternation of the retinal, which is defined as the average of the lengths of the single bonds minus that of the double bonds of the C5–N moiety.

Relative to the gas phase, the interaction of the retinal with the counterion (Glu113 in vertebrates, Glu180 in invertebrates) induces a strong blue shift of ~ 120 nm and moves the calculated λ_{max} very close to the experimental value of 500 nm for 11-*cis*-rhodopsin.²⁵ The shift is conceivable because the excited-state charge density is shifted against the charge of the counterion, leading to a change in the dipole moment $\Delta\mu_{S_1-S_0^*}$, which was calculated to be ~ 12.0 D for all of the retinal isomers in pigments, in excellent agreement with the experimental measurements of Mathies et al.²⁶ Similarly, the difference between the ground-state dipole moments in going from the gas phase to the protein environment ($\Delta\mu_{S_0}^{\text{R-S}}$) was calculated to be ~ 6.5 D. This value is almost equal to the value of 6.8 D calculated for all-*trans*-retinal in the gas phase and bacteriorhodopsin.²⁷

In the absence of electrostatic interactions with the counterion, the calculated λ_{max} was found to be ~ 600 nm, which is almost equal to that found in the gas phase.²⁸ Apparently, effect of the neutral residues lining the binding pocket is negligible in comparison with the strong effect of the counterion, as originally predicted by mutagenesis studies more than 20 years ago.⁴ The negative and positive twists about the C11=C12 and C12–C13 bonds impart a positive helicity²⁹ to all of the *cis*-PSBRs. The spectral manifestation of the twist is evident in the calculated rotatory strengths (R), which are positive in sign and undergo a slight increase in magnitude as the retinal enters the protein from the gas phase. Of all the retinal isomers in the protein, the least stable isomer, PSB7, has the largest oscillator strength ($\Delta f = 1.59$) and rotatory strength ($\Delta R = 0.41$), while the most stable isomer, PSB11, has the smallest values ($\Delta f = 1.32$, $\Delta R = 0.19$).

We also found an interesting correlation between the PSB7 and PSB11 isomers. In the case of squid, the Schiff base NH bond

Table 2. SORCI+Q-Calculated Average Values of the $S_0 \rightarrow S_1$ Absorption Wavelength ($\Delta\lambda$, nm), Oscillator Strength (Δf), Rotatory Strength (ΔR , au), and Dipole Moments ($\Delta\mu$, D) for All of the PSBR Isomers in Vertebrate (Bovine, Monkey) and Invertebrate (Squid) Pigments

PSBR	gas phase (QM only)		protein (QM/MM)				
	$\Delta\lambda$	Δf	$\Delta\lambda$	Δf	ΔR	$\Delta\mu_{S_1-S_0}$	$\Delta\mu_{S_0}^{P-S}$
PSB7	553	1.20	431	1.59	0.41	12.1	6.00
PSB9	566	1.20	456	1.42	0.23	11.7	6.32
PSB11	611	1.10	490	1.32	0.19	11.7	6.95
PSB13	623	1.27	508	1.45	0.17	12.5	6.43

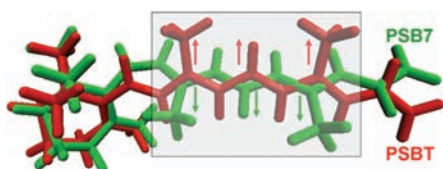


Figure 4. Overlay of PSB7 (green) and PSBT (red).

that was originally oriented toward Y111 in rhodopsin was found to be reoriented toward N87 in 7-*cis*-rhodopsin. Apparently, a similar structural rearrangement was also found in the QM/MM³⁰ and X-ray³¹ structures of squid bathorhodopsin. Although the Schiff base environments of PSB7 and PSBT are identical in squid rhodopsin, the geometric and spectroscopic properties of these two isomers were found to be opposite to each other. In PSBT, the C9 and C13 methyl groups point upward, whereas in PSB7 they point downward. Further, a red shift of ~ 50 nm separates bathorhodopsin (~ 540 nm) from rhodopsin (~ 490 nm), whereas a blue shift of ~ 50 nm separates 7-*cis*-rhodopsin (~ 440 nm) from rhodopsin (~ 490 nm). While the red shift is attributed to twisting of the double bonds in PSBT, the blue shift is attributed to twisting of the single bonds in PSB7. Therefore, we suggest that PSB7 is an “upside-down” version of PSBT (Figure 4).

In conclusion, the present study not only enables us to answer why nature selects 11-*cis*-retinal but also helps us to understand why 7-*cis*-, 9-*cis*-, and 13-*cis*-retinal are not found in the eye. Although factors such as accessibility of the retinal to enzymatic biosynthesis, physiological stability, rate of binding, quantum yield, and stereoselectivity of the photoisomerization are critical, it remains to be seen how far the evidence presented in this communication can aid in optimizing the parameters required for the natural selection of the light-sensing chromophore. As the strength of rhodopsin appears to lie in the selection of 11-*cis*-retinal, reducing this strength to enhance the weakness of accommodating other retinal isomers is not the goal pursued by evolution.

■ ASSOCIATED CONTENT

Supporting Information. Cartesian coordinates of all the retinal models discussed in this study and complete refs 3a, 9, 10b, 11, 19, 27, and 28. This material is available free of charge via the Internet at <http://pubs.acs.org>.

■ AUTHOR INFORMATION

Corresponding Author
morokuma@emory.edu

■ ACKNOWLEDGMENT

The authors thank Prof. H. Kandori and Kota Katayama for valuable discussions during the preparation of monkey rhodopsin and A. Altun, H. Hirao, and L. W. Chung for their technical assistance. The work at Emory was supported in part by a grant from the National Institutes of Health (R01EY016400) and the work at Kyoto by a Core Research for Evolutional Science and Technology (CREST) Grant in the Area of High Performance Computing from JST.

■ REFERENCES

- (1) Birge, R. R. *Annu. Rev. Biophys. Bioeng.* **1981**, *10*, 315.
- (2) Terakita, A.; Yamashita, T.; Tachibana, S.; Shichida, Y. *FEBS Lett.* **1998**, *439*, 110.
- (3) (a) Palczewski, K.; et al. *Science* **2000**, *289*, 739. (b) Murakami, M.; Kouyama, T. *Nature* **2008**, *453*, 363.
- (4) Sakmar, T. P.; Franke, R. R.; Khorana, H. G. *Proc. Natl. Acad. Sci. U.S.A.* **1989**, *86*, 8309.
- (5) Sekharan, S.; Altun, A.; Morokuma, K. *Chem.—Eur. J.* **2010**, *16*, 1744.
- (6) (a) Degrip, W. J.; Liu, R. S. H.; Ramamurthy, V.; Asato, A. *Nature* **1976**, *262*, 416. (b) Maeda, A.; Shichida, Y.; Yoshizawa, T. *J. Biochem.* **1978**, *83*, 661.
- (7) Schick, G. A.; Cooper, T. M.; Holloway, R. A.; Murray, L. P.; Birge, R. R. *Biochemistry* **1987**, *5*, 2556.
- (8) Kligler, D. S.; Horwitz, J. S.; Lewis, J. W.; Einterz, C. M. *Vision Res.* **1978**, *24*, 1465.
- (9) Sekharan, S.; et al. *J. Am. Chem. Soc.* **2007**, *129*, 1052.
- (10) (a) Crouch, R.; Purvin, V.; Nakanishi, K.; Ebrey, T. *Proc. Natl. Acad. Sci. U.S.A.* **1975**, *72*, 1538. (b) Shichida, Y.; et al. *Biochemistry* **1988**, *27*, 6495.
- (11) (a) Harbison, G. S.; et al. *Proc. Natl. Acad. Sci. U.S.A.* **1984**, *81*, 1706. (b) Sasaki, J.; et al. *Science* **1995**, *269*, 73.
- (12) (a) Birge, R. R.; Sullivan, M. J.; Kohler, B. E. *J. Am. Chem. Soc.* **1976**, *98*, 358. (b) Nakanishi, K. *Am. Zool.* **1991**, *31*, 479.
- (13) (a) Warshel, A. *Nature* **1976**, *260*, 679. (b) Schoenlein, R. W.; Peteanu, L. A.; Mathies, R. A.; Shank, C. V. *Science* **1991**, *254*, 412.
- (14) Warshel, A.; Levitt, M. *J. Mol. Biol.* **1976**, *103*, 227.
- (15) Vreven, T.; Morokuma, K.; Farkas, O.; Schlegel, H. B.; Frisch, M. J. *J. Comput. Chem.* **2003**, *24*, 760.
- (16) Altun, A.; Yokoyama, S.; Morokuma, K. *J. Phys. Chem. B* **2008**, *112*, 6814.
- (17) Oprian, D. D.; Asenjo, A. B.; Lee, N.; Pelletier, S. L. *Biochemistry* **1991**, *30*, 11367.
- (18) Birge, R. R.; Einterz, C. M.; Knapp, H. M.; Murray, L. P. *Biophys. J.* **1988**, *53*, 367.
- (19) (a) Delange, F.; et al. *Biochemistry* **1998**, *37*, 1411. (b) Verdegem, P. J. E.; et al. *Biochemistry* **1999**, *38*, 11316.
- (20) Vreven, T.; Morokuma, K. *Annu. Rep. Comput. Chem.* **2006**, *2*, 35.
- (21) Kochendoerfer, G. G.; Verdegem, P. J. E.; van der Hoef, I.; Lugtenburg, J.; Mathies, R. A. *Biochemistry* **1996**, *35*, 16230.
- (22) Amora, T. L.; Ramos, L. S.; Galan, J. F.; Birge, R. R. *Biochemistry* **2008**, *47*, 4614.
- (23) deGrip, W. J.; Bovee-Geurts, P. H.; Wang, Y.; Verhoeven, M. A.; Lugtenburg, J. *J. Nat. Prod.* **2011**, *74*, 383.
- (24) Neese, F. A. *J. Chem. Phys.* **2003**, *119*, 9428.
- (25) (a) Gascon, J. A.; Batista, V. S. *Biophys. J.* **2004**, *87*, 2931. (b) Sekharan, S.; Sugihara, M.; Buss, V. *Angew. Chem., Int. Ed.* **2007**, *46*, 269.
- (26) Mathies, R.; Stryer, L. *Proc. Natl. Acad. Sci. U.S.A.* **1976**, *73*, 2169.
- (27) Hoffmann, M.; et al. *J. Am. Chem. Soc.* **2006**, *128*, 10808.
- (28) Andersen, L. H.; et al. *J. Am. Chem. Soc.* **2005**, *127*, 12347.
- (29) Shichida, S.; Tokunaga, F.; Yoshizawa, T. *Biochim. Biophys. Acta* **1978**, *504*, 413.
- (30) Sekharan, S.; Morokuma, K. *J. Am. Chem. Soc.* **2011**, *133*, 4734.
- (31) Murakami, M.; Kouyama, T. *J. Mol. Biol.* **2011**, *453*, 363.